Dimensionality effects on the Holstein polaron

Li-Chung Ku,[1,2] S. A. Trugman,[1] and J. Bonča[3]
[1]*Theoretical Division, Los Alamos National Laboratory, Los Alamos, New Mexico 87545*
[2]*Department of Physics, University of California, Los Angeles, California 90024*
[3]*FMF, University of Ljubljana and J. Stefan Institute, 1000, Ljubljana, Slovenia*
(Received 14 September 2001; published 29 April 2002)

Based on a recently developed variational method, we explore the properties of the Holstein polaron on an infinite lattice in D dimensions, where $1 \leqslant D \leqslant 4$. The computational method converges as a power law, so that highly accurate results can be achieved with modest resources. We present the most accurate ground state energy (with no small parameter) to date for polaron problems, 21 digits for the one-dimensional (1D) polaron at intermediate coupling. The dimensionality effects on polaron band dispersion, effective mass, and electron-phonon (el-ph) correlation functions are investigated in all coupling regimes. It is found that the crossover to large effective mass of the higher-dimensional polaron is much sharper than the 1D polaron. The correlation length between the electron and phonons decreases significantly as the dimension increases. Our results compare favorably with those of the quantum Monte Carlo, dynamical mean-field theory, density-matrix renormalization-group, and Toyozawa variational methods. We demonstrate that the Toyozawa wave function is qualitatively correct for the ground-state energy and the two-point electron-phonon correlation functions, but fails for the three-point functions. Based on this finding, we propose an improved Toyozawa variational wave function.

DOI: 10.1103/PhysRevB.65.174306 PACS number(s): 74.20.Mn, 74.25.Kc

I. INTRODUCTION

The Holstein model, as a paradigm for polaron formation, has attracted renewed interest in recent years because several lines of experimental evidence support the presence of polaron carriers in strongly correlated electronic materials, including colossal magnetoresistance manganites,[1] organics,[2] quasi-one-dimensional systems, and high-T_c cuprates.[3,4] Theoretical research on polaron physics began six decades ago, and the problem remains unsolved due to its intrinsic many-body complexity from the electron-phonon (el-ph) interaction. (The problem of excitons coupled to phonons is formally equivalent.[5]) Standard perturbation treatments[6,7] are usually limited to a particular parameter regime. With constantly growing computational resources, various numerical techniques have been applied to polaron problems in recent years, which give the most reliable results in the physically interesting crossover regime. These techniques include finite-cluster exact diagonalization (ED),[8–13] the quantum Monte Carlo (QMC) method,[14,15] the density-matrix renormalization group (DMRG) method,[16] and the global-local variational method (GLVM).[17]

Recent numerical studies have focused on the one-dimensional (1D) lattice model. Due to the enormous phonon Hilbert space in three dimensions, the dimensionality effects on the polaron problems are less studied except in the adiabatic (or semiclassical) approximations,[18,19] and in perturbation theory.[20] The QMC method is also capable of computing the energy and effective mass of the 3D polaron, but the full dispersion $E(\vec{k})$ is only reliable in the strong-coupling regime. However, with a recently developed variational method, we can compute the polaron effective mass, band dispersion, and el-ph correlation functions of the ground and low-lying excited states in all coupling regimes, preserving the full quantum dynamical feature of phonons (details can be found in Ref. 21). The variational space is defined on an infinite lattice, although only a finite separation is allowed between the electron and the surrounding phonons in current implementations. We systematically expand the variational space so that highly accurate results can be achieved with modest computational resources.

The main purpose of this paper is to characterize the Holstein polaron in higher dimensions. We consider a single-electron Holstein Hamiltonian on a D-dimensional hypercubic lattice,

$$\begin{aligned} H &= H_{el} + H_{el\text{-}ph} + H_{ph} \\ &= -t \sum_{\langle i,j \rangle} (c_i^\dagger c_j + \text{H.c.}) - \lambda \sum_j c_j^\dagger c_j (a_j + a_j^\dagger) \\ &\quad + \omega \sum_j a_j^\dagger a_j , \end{aligned} \tag{1}$$

where $c_j^\dagger$ creates an electron and $a_j^\dagger$ creates a phonon on site j. The parameters of the model are the nearest-neighbor hopping integral t, the el-ph coupling strength λ, and the phonon frequency ω. The electron is coupled locally to a dispersionless optical phonon mode.[22] There are two commonly defined dimensionless control parameters, the adiabaticity ratio $\gamma = \omega/t$ and the el-ph coupling strength $\alpha = E_p/2Dt$, which is defined as the ratio of polaron energy for an electron confined to a single site $E_p = \lambda^2/\omega$ and the free electron half bandwidth $2Dt$. The strong- (weak-) coupling regime refers to $\alpha > 1$ (<1), and the adiabatic (antiadiabatic) regime refers to $\gamma < 1$ (>1). An additional dimensionless parameter is $g = \lambda/\omega$, which appears in strong-coupling perturbation theory.

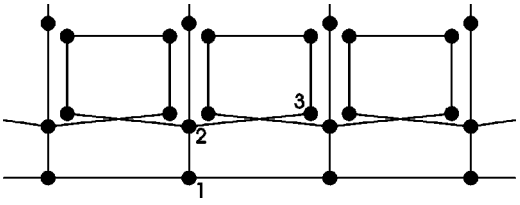

FIG. 1. A small variational Hilbert space, a subset of the generation 3 space, is shown for the 1D polaron. Basis states in the many-body Hilbert space are represented by dots, and nonzero off-diagonal matrix elements by lines. State $|1\rangle$ in the root state, an electron at the origin with no phonon excitations. Vertical bonds create or destroy phonons. State $|2\rangle$ is an electron and one phonon, both at the origin. State $|3\rangle$ is an electron on site 1, and a phonon on site 0. The dots can also be thought of as Wannier orbitals in a one-body periodic tight-binding model.

A variational space is constructed beginning with a root state, the electron at the origin with no phonon excitations, and acting repeatedly with the off-diagonal terms (t and λ) in the Hamiltonian [Eq. (1)]. States in generation m are those that can be created by acting m times with off-diagonal terms. All translations of these states on an infinite lattice are included, and the problem is diagonalized for a given momentum $\vec{k}$ using a Lanczos method.[21] A small variational space, with seven states per electron site (unit cell), is shown in Fig. 1. (The more accurate numerical computations are done with over 10^7 states per unit cell.)

The total number of states N_{st} per unit cell after m generations increases exponentially approximately as $(D+1)^m$, where D is the spatial dimension. [The bipolaron has the same $(D+1)^m$ dependence, but with a larger prefactor.] The perhaps surprising fact is that while the size of the Hilbert space grows exponentially with m, the error in the ground-state energy decreases exponentially, because states are added in a fairly efficient order. Figure 2 shows the fractional error in the ground-state energy as a function of the number of basis states in Hilbert space. The accuracy is determined by comparing the energy as the size of the Hilbert space is increased. At intermediate coupling in any dimension, the energy improves by about a factor of 8 with each generation.[23] In one dimension, each added generation approximately doubles the size of the Hilbert space, whereas in four dimensions, the size increases fivefold. This rapid convergence at intermediate-coupling is valuable since no analytic approach is reliable in this regime. Table I lists the energies for 1D to 4D polarons at intermediate to weak coupling. The accuracy, 21 digits for a 1D polaron, is high compared to that of other numerical methods, such as two or three digits for QMC, six digits for DMRG (or GLVM), and up to eight digits for ED.[24] Moreover, for the 3D polaron at intermediate to strong coupling, an energy accuracy of $8-10$ decimal places can be achieved in the nonadiabatic regime with fewer than 3×10^6 basis states. To obtain an accuracy beyond 13 digits, the code is executed in quadruple precision. The present variational method requires only power-law time to achieve a given accuracy (in any dimension),

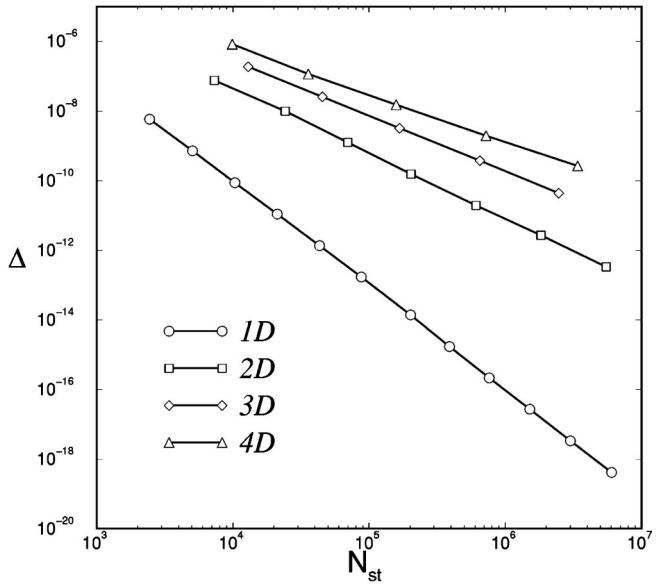

FIG. 2. The fractional error Δ in the polaron ground-state energy as a function of the number of basis states N_{st} in the Hilbert space for parameters $\alpha=0.5$, $g=1.0$, and $t=1.0$.

which is a qualitative improvement on exact diagonalization as it is currently implemented, the latter requiring exponential time.

In this paper we present detailed studies of the dimensionality effect on the Holstein polaron. First of all, we explore the polaron characteristics in the $k=0$ ground state, and compare our results with previous studies from QMC, DMRG, and dynamical mean-field theory (DMFT). Second, we compute the el-ph correlation function and the polaron energy $E(\vec{k})$. Finally, the validity of the Toyozawa variational method is investigated by calculating the ground-state energy, and the two- and three-point el-ph correlation functions.

II. SMALL-POLARON CROSSOVER

A. Quasiparticle weight Z_k and effective mass m^*

The small polaron crossover or ''self-trapping transition'' has been one of the core issues in polaron problems. Adiabatic theory suggests that the polaron in two and three dimensions (but not in one dimension), is in an ''extended'' state with an infinite radius below an el-ph coupling threshold λ_c, and beyond which is a ''localized'' state with infinite effective mass. (This phenomenon is usually termed the ''self-trapping transition.'') However, our studies confirm that in all dimensions, there is a crossover rather than a self-trapping transition (ground-state properties are analytic), if the parameters are finite. This result is consistent with some other recent studies,[20,14] and corroborates the theorem of Gerlach and Löwen.[25]

The quasiparticle weight (renormalization factor) is defined by the overlap (squared) between the bare electron and a polaron, i.e.,

$$Z_k=|\langle\Psi_{0,k}|c_k^\dagger|0\rangle|^2, \tag{2}$$

in which $|\Psi_{0,k}\rangle$ is the ground-state wave function of a polaron and $|0\rangle$ is the vacuum state. Z_k can be measured in photoemission or tunneling experiments. Figure 3 shows the

TABLE I. Polaron ground state energies at $k=0$ in one to four dimensions (1D–4D) for $\alpha=0.5$, $g=1.0$, and $t=1.0$.

	1D	2D	3D	4D
E_0	-2.46968472393287071561	-4.814735778337	-7.1623948409	-9.513174069

crossover of $Z_{\vec{k}=0}$ as a function of $1/\alpha$ at $g=3$, for 1D–4D cases. We see that *the crossover to large effective mass (large* z^{-1}*) of the higher-dimensional polaron is much sharper than the* 1*D polaron*. For $D>1$, a fairly abrupt crossover occurs at $\alpha>1$, whereas the crossover for the 1D polaron spans a wide range of α. With a smaller g (but greater than 1), the crossover will be slower but with the same dimensional characteristics. In the limit $1/\alpha\rightarrow 0$, the phonon wave function contracts to the electron site, with $Z_k=\exp(-g^2)$. The inset shows a comparison of Z_k and m_0/m^* for the 1D polaron. Their fractional difference δ, defined as $(m_0/m^*-Z_k)/Z_k$, is shown as a dotted line. The maximum δ is 22%, in the intermediate coupling regime, while the minimum occurs as $1/\alpha\rightarrow 0$ (small t), where δ is the order of t^2 from strong-coupling perturbation theory (SCPT). We find that δ decreases significantly as the dimension increases. The maximum difference δ_{max} is 4.5% for the 2D polaron and 2.0% for the 3D polaron. For $g=\sqrt{5}$, δ_{max} in three dimensions drops to 0.63%.

The ground-state energy E satisfies $E=\epsilon_0-2t\cos(k)+\Sigma(k,E)$, where $\Sigma(k,E)$ is the self-energy. $Z_{k=0}$ is the probability of the wave function on the root site, and from first-order perturbation theory $Z_{k=0}=\partial E/\partial\epsilon_0$, resulting in $Z_{k=0}=1/[1-\partial\Sigma(k,E)/\partial E]$. The origin of the difference between the inverse mass and $Z_{k=0}$ lies in the k dependence of the self-energy,

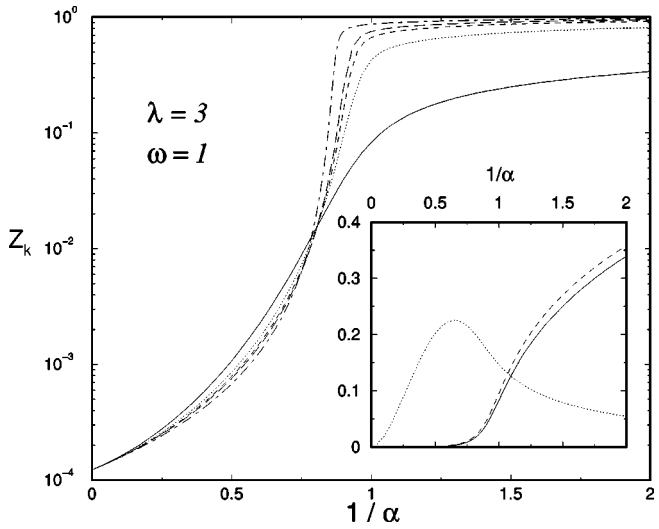

FIG. 3. Quasiparticle weight $Z_{\vec{k}=0}$ as a function of the inverse coupling strength $1/\alpha$ for one (solid line), two (dotted line), three (dashed line), and four (long dashed line) dimensions. α is varied by changing the hopping t at fixed ω and λ. The comb basis approximation (see below) is shown as a dot-dashed line. The inset shows the comparison of the inverse effective mass m_0/m^* (dashed line) and Z_k (solid line) for one dimensions. The fractional difference $\delta=(m_0/m^*-Z_k)/Z_k$ is plotted as a dotted line.

$$\frac{m_0}{m^*}-Z_{k=0}=\frac{1}{2t}\frac{\partial^2\Sigma(k,E)}{\partial k^2}\Bigg/\left(1-\frac{\partial\Sigma(k,E)}{\partial E}\right), \qquad (3)$$

where the derivatives are evaluated at the ground state energy $E=E_0$ and $k=0$. In the variational space of Fig. 1 or in the full space, the self-energy has a nonzero k dependence because distinct unit cells are connected at branch level (path $1-2-3\ldots$), in addition to the trivial connection at root level. A restricted variational space, the comb basis, allows phonon excitations only on the electron site, as shown in Fig. 4. In this subspace, the self-energy is k independent, since the only path between unit cells is at the root level. The self-energy remains k independent even in a larger space in which the tree trunks sprout lateral branches, so long as the branches do not connect to neighboring unit cells. For these cases, the Z factor and inverse mass are identical, $\delta=0$. In $O(t)$ SCPT, δ vanishes for the same reason and $Z_{k=0}=m_0/m^*=\exp(-g^2)$.

The effect of dimensionality on δ is made plausible by the following. In the Holstein model, the dimensionality D does not directly affect the term $H_{el\text{-}ph}$ in Eq. (1), because the el-ph coupling is local and the phonon is dispersionless. High-dimensional polarons share the same simplicity of the el-ph coupling as 1D polarons. Furthermore, we see (in Sec. III) that the el-ph correlation length decreases as D increases. Thus the k dependence of the self-energy weakens in higher dimensions. The above arguments do not, however, hold for the Fröhlich model (or the extended Holstein model) with longer-range el-ph coupling,[26–28] where Z_k and m_0/m^* behave quite differently.

B. Comparison with QMC, DMRG, and DMFT methods

Figure 5 shows our results for the effective mass as a function of α (at fixed $\gamma=1.0$) in comparison with DMRG and QMC. Our results are accurate to at least four digits,

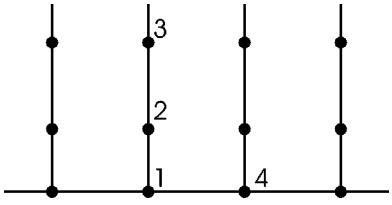

FIG. 4. The comb basis, a variational space in which phonon excitations are present only on the electron site. Vertical lines create phonons and horizontal lines are the electron hops. State $|1\rangle$ is an electron on site 0 and no phonons. State $|2\rangle$ is an electron and one phonon, both on site 0. State $|3\rangle$ is an electron and two phonons, all on site 0. State $|4\rangle$ is the translation of state $|1\rangle$. The comb basis is a subset of the larger variational space. As in DMFT, it only keeps track of the on-site el-ph correlations.

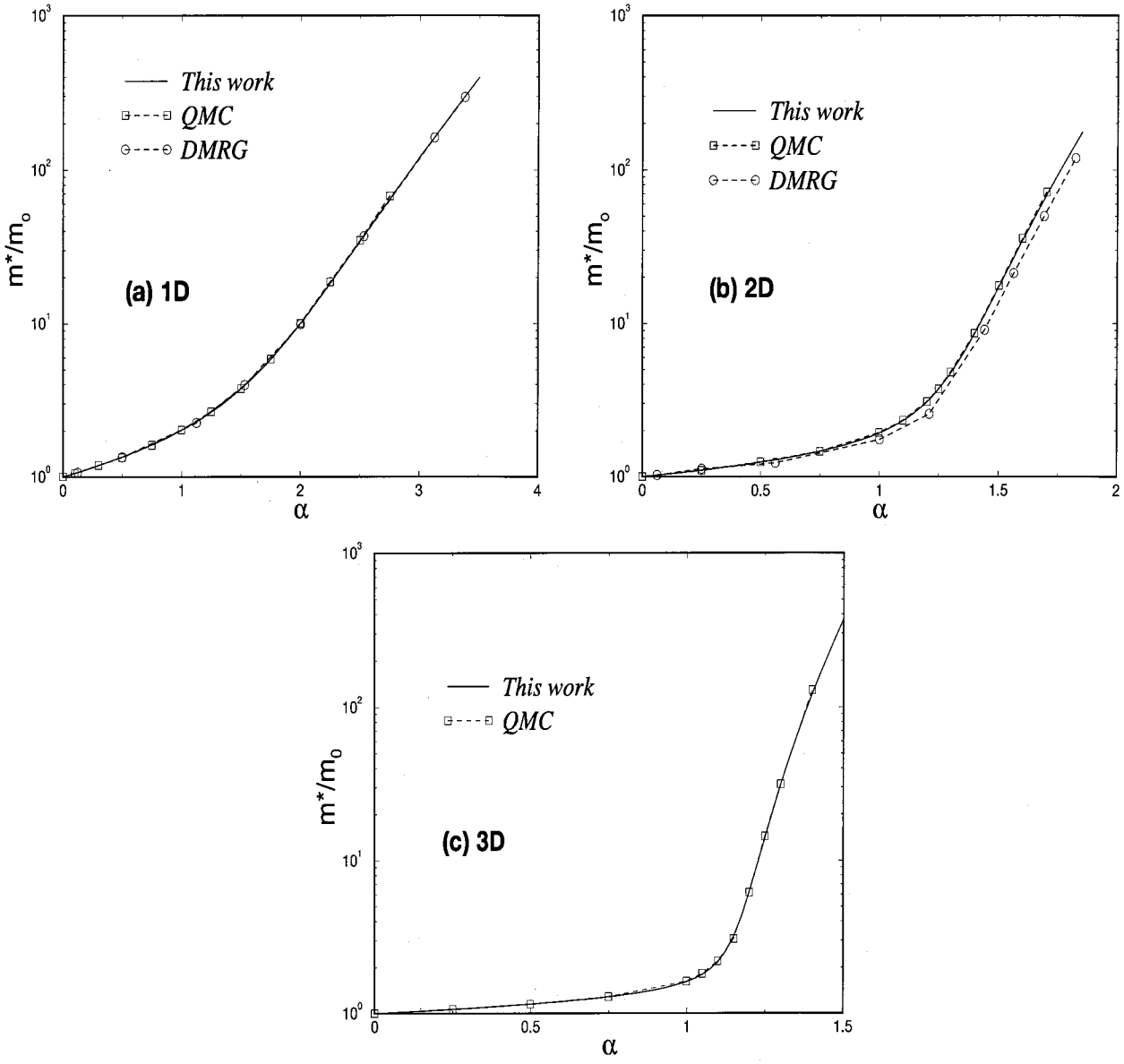

FIG. 5. The effective mass m^* for the (a) 1D, (b) 2D, and (c) 3D polarons is compared to DMRG (Ref. 16) and QMC (Ref. 14) calculations. (No DMRG data are available for the 3D polaron.) In all cases, $\omega=1.0$, and $t=1.0$. Note the different horizontal scales.

which is well below the linewidth. In all cases [Figs. 5(a)–5(c)], m^*/m_0 increases slowly when α is small, followed by a rapid increase when $\alpha>1$. Since it is calculated at $\omega=t=1.0$ (not a small t), the mass behaves differently than $\exp(g^2)$ that SCPT suggests. Note that the crossover is more rapid as D increases, which is consistent with the results in Sec. II A. In every dimension, our results are in quantitative agreement with QMC. The numerical error in QMC is approximately 0.1% to 0.3%,[14] which is good though less accurate than finite cluster ED or the present approach. DMRG is generally considered a powerful tool in dealing with many-body problems. Using DMRG, Jeckelmann and White have calculated Holstein polaron properties in 1D and 2D. DMRG seems to be most successful in calculating the ground-state energy (at $k=0$) and el-ph correlation functions. However, finite-size scaling is required for DMRG to compute m^*,[16] which becomes more difficult for $D>1$. In 1D [Fig. 5(a)] the results from DMRG are as accurate as those from QMC. DMRG does not, however, calculate the mass accurately in 2D [Fig. 5(b)].

Dynamical mean-field theory has previously been applied to the Holstein polaron problem.[29] The approach is exact in infinite dimensions but an interpolation to 3D lattices is made possible by using a semielliptical free density of states $N(E)$ to mimic the low-energy features. Figure 6 shows a comparison of our results on a cubic lattice to DMFT, which is made by setting the bandwidths equal. Overall, in panel (a), we see a qualitative agreement between the two calculations. DMFT is accurate in the strong-coupling regime, where the surrounding phonons are predominately on the electron site. This is also the regime where strong-coupling perturbation theory works well. In Fig. 6(b), we see our numerical results in agreement with weak-coupling perturbation theory in λ. However, DMFT fails to compute m^* cor-

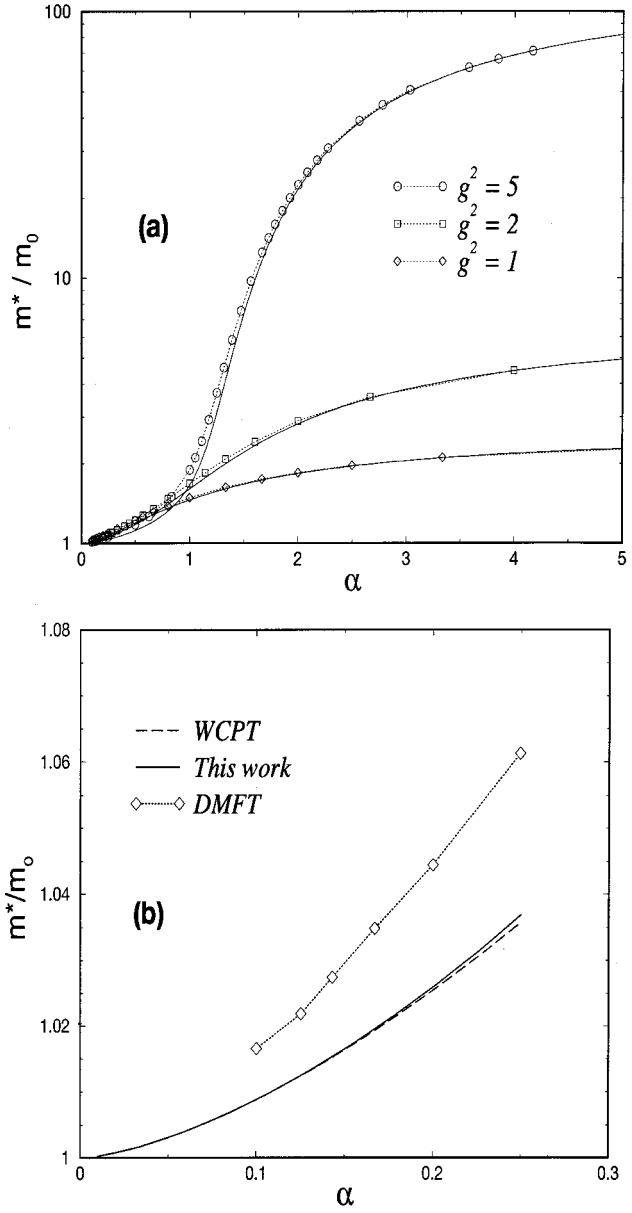

FIG. 6. (a) The mass m^* of the 3D polaron, $\omega=1$, this work (solid lines) compared to DMFT (dotted lines) (Ref. 29). (b) Comparison to weak-coupling perturbation theory (WCPT) for $g^2=5$.

rectly in the weak-coupling regime. The reason is that, in DMFT, the lattice problem is mapped onto a self-consistent local impurity model,[30,31] which preserves the interplay of the electron and the phonons only *at the local level*. We will see that the spatial extent of the el-ph correlations increases as the el-ph coupling decreases, which explains the significant discrepancy in the weak-coupling regime. It is also worth noting that DMFT neglects the k dependence of self-energy, i.e., the inverse effective mass is always equal to the quasiparticle weight. As we have pointed out above, the difference between m_0/m^* and Z_k is not negligible in the intermediate- to weak-coupling regime.

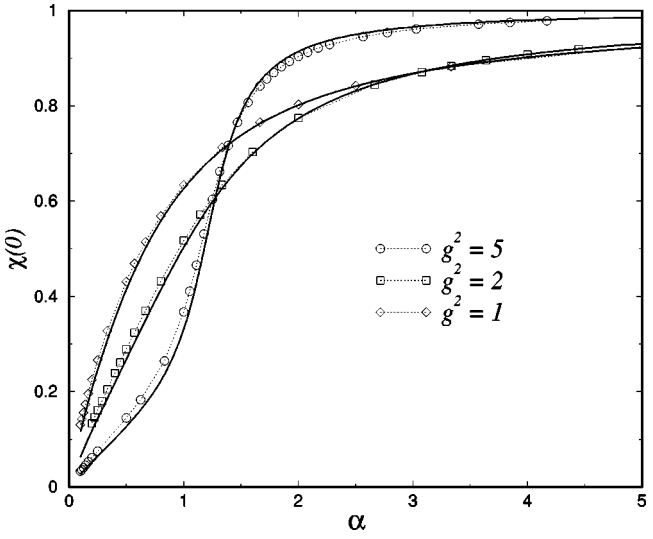

FIG. 7. The on-site correlation $\chi(0)$ for the 3D polaron. Our results (solid lines) are compared to the DMFT (dotted lines with symbols). The parameters are the same as in Fig. 6

III. ELECTRON-PHONON CORRELATIONS

Next we compute the correlation function between the electron and phonon displacements (lattice deformation) in the ground state:

$$\chi(i-j)=\langle\Psi_0|c_i^\dagger c_i(a_j+a_j^\dagger)|\Psi_0\rangle. \tag{4}$$

This correlation function can be considered as a measure of the polaron size.[32] It should not be confused with the ''polaron radius'' in the extreme adiabatic limit, which refers to the spatial extent of a symmetry-breaking localized state. We would like to emphasize that a comprehensive study of el-ph correlation for the ground state of the 3D polaron has not yet been reported by any other modern numerical technique,[33] to our knowledge. The *on-site correlation* has been studied by DMFT, and the results are compared in Fig. 7.[34] The on-site lattice distortion $\chi(0)$ is shown as function of α and the rest of parameters are the same as in Fig. 6. In Fig. 7, $\chi(0)$ is normalized to 1 when α is infinite (i.e., $t\to 0$) according to $\lim_{t\to 0}\chi(0)=2g$. Again, we obtain a good qualitative agreement. The curves show an abrupt change in slope only for large g, where the discrepancy with DMFT is largest.

Figure 8 shows the effect of dimensionality on the correlation function $\chi(i-j)$. In the strong-coupling regime, panel (a) shows, in every dimension, a sharp drop on the first two sites and an exponentially decaying tail. For the 3D polaron at a distance of three lattice sites, $\chi(3)/\chi(0)$ drops below 10^{-4}. In the weak-coupling regime [panel (b)] χ has nearly a simple exponential decay with a less steep slope, which implies a nontrivial extent of the el-ph interplay in space. In both panels, we observe a common trend that χ decays more rapidly as the lattice dimension increases, i.e., the surrounding phonons are more localized near the electron in higher dimensions. This feature enables DMFT to give sensible results in higher finite dimensions. We have also investigated

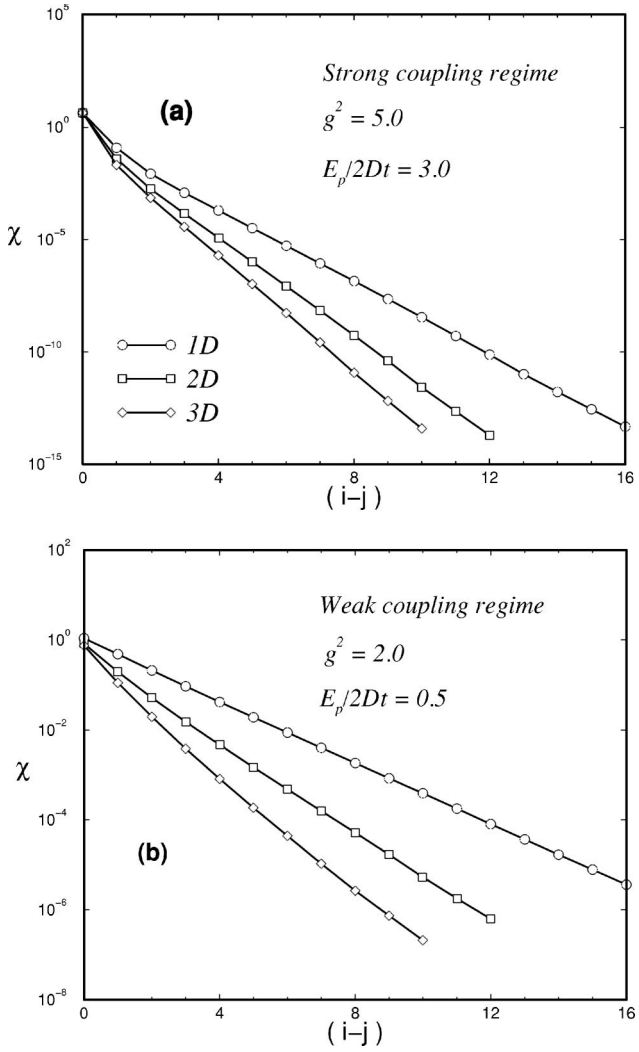

FIG. 8. Correlation χ of the electron density and the phonon displacement as a function of distance $(i-j)$ for the 3D polaron along the (1,0,0) direction, the 2D polaron along the (1,0) direction, and the 1D polaron at (a) strong coupling, and (b) weak coupling, $\omega=1.0$. Note the different vertical scales.

other two-point el-ph correlation functions such as $\langle c_i^\dagger c_i a_j^\dagger a_j\rangle$ (not shown), which has dimensional characteristics similar to χ.

The rapid decay of the el-ph correlation function for the higher-dimensional polaron suggests that the off-site el-ph interplay is relatively weak in large D. One would then expect the comb basis of Fig. 4, a subspace of the full Hilbert space, to give a better approximation in large D. We check this assumption by numerically calculating the fraction of the probability density in the exact ground state that resides in the comb subspace,

$$P_{comb}=\langle\Psi_0|\hat{P}|\Psi_0\rangle, \tag{5}$$

where $\hat{P}$ is the projection operator onto the comb subspace and the wave function Ψ_0 is obtained in the full variational space. Figure 9 shows P_{comb} as a function of the inverse bare coupling constant $1/\alpha$ for 1D–4D cases. In both of the limits

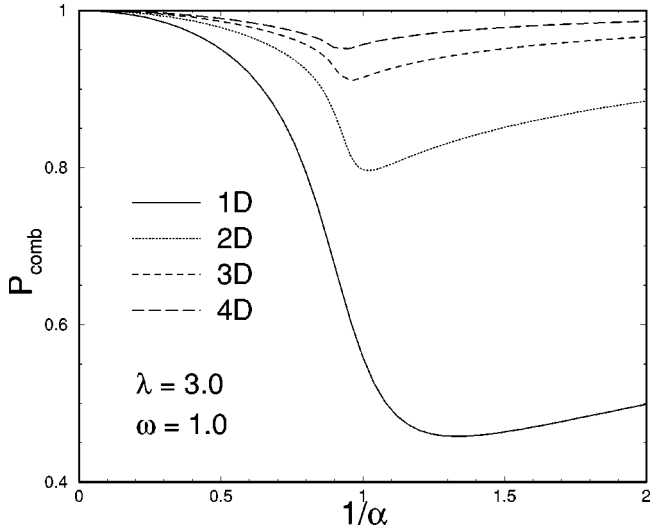

FIG. 9. The probability density in the ground state that resides in the comb subspace P_{comb} as a function of the inverse bare coupling strength $1/\alpha$, for the 1D-4D polaron. The parameter set is the same as in Fig. 3.

$\alpha=0$ or $\alpha=\infty$, P_{comb} goes to 1. The minimum overlap occurs in the crossover regime. As expected, P_{comb} gets closer to 1 as D increases. For the 3D polaron, the minimum of P_{comb} is 91.1%, in contrast to 45.8% for the 1D polaron. These trends can also be seen analytically. In the adiabatic limit ($\omega=0$), perturbing in t from a self-trapped state with energy E_p, the self-trapping transition occurs at $\alpha=1-1/(4D)$. The leading order correction of P_{comb} for the self-trapped polaron state is

$$\Delta_{comb}\equiv 1-P_{comb}=\frac{1}{8D\alpha^2}. \tag{6}$$

In the nonadiabatic limit, Δ_{comb} can be calculated by SCPT to second order in the hopping t. It takes the following form:

$$\Delta_{comb}=\frac{g^4 e^{-2g^2}}{2D\alpha^2}\sum_{n=0}^{\infty}\sum_{m=1}^{\infty}\frac{g^{2(n+m)}}{n!m!}\frac{1}{(n+m)^2}. \tag{7}$$

The above expressions show that for a given α and g, the discrepancy Δ_{comb} decreases as D increases and eventually vanishes in infinite D. The comb basis should thus give a good account for the Holstein problem in large D. We see in Fig. 3, however, that dimension 3 is not high enough for the comb to give quantitatively accurate results, and that dimension 4 is not much better. Convergence to higher dimensions is slow.

IV. ENERGY DISPERSION $E(\vec{k})$

Most of the recently developed numerical methods are capable of computing the polaron band dispersion in 1D. For the 2D polaron, the only nonperturbative calculations of band dispersion published so far were computed by finite-cluster ED (Ref. 11) and quantum Monte Carlo methods.[15] Due to the huge phonon Hilbert space in high dimensions, the previous ED results are limited to small clusters, so that

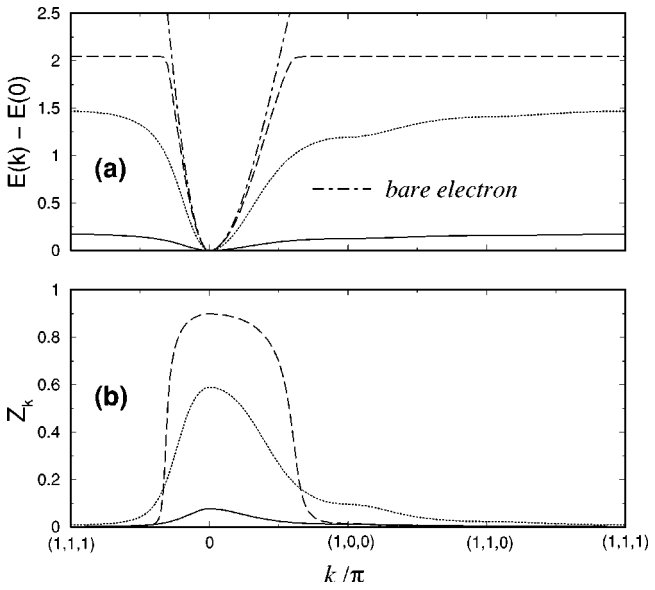

FIG. 10. Ground state energy $E(\vec{k})$ of the 3D polaron in panel (a) and quasiparticle weight Z_k in panel (b) for three different el-ph coupling constants: $\lambda=4.5$ (solid line), $\lambda=3.5$ (dotted line), and $\lambda=2.0$ (dashed line). The other parameters are $\omega=2.0$ and $t=1$. The dot-dashed line in (a) is the dispersion of a bare electron. The corresponding ground-state energies $E(\vec{k}=0)$ are -10.608348, -8.0642850, and -6.588526818, respectively.

the band dispersion can only be evaluated at a few $\vec{k}$ points. The QMC allows calculation of energy at any desired $\vec{k}$ point, but is limited to the condition that the polaron bandwidth is much smaller than the phonon frequency, which corresponds to the strong-coupling regime.

The present variational approach, however, is not subject to any of the above restrictions.[21] Figure 10(a) shows the evolution of the band dispersion for a 3D polaron along symmetry directions in the Brillouin zone at various el-ph coupling constants λ. Figure 10(b) shows the corresponding Z_k. Starting with weak coupling $\lambda=2.0$ (dashed line), the polaron band is close to the bare electron band at a lower band edge. The deviation between them increases as $\vec{k}$ increases. When $E(k)-E(0)$ approaches ω, we observe a band flattening effect, similar to the 1D and 2D cases, accompanied by a sharp drop of quasiparticle weight Z_k. The large-k lowest-energy state can be considered roughly as ''a $k=0$ polaron ground state'' plus ''an itinerant (or weakly bound) phonon with momentum k.'' It is the phonon that carries the momentum, so as to make Z_k essentially vanish and to give a bandwidth $E(\pi)-E(0)\approx\omega$. Due to the large extent of the el-ph correlations in the flattened band, our results are less accurate in the flattened regime.[35] In the case of intermediate coupling $\lambda=3.5$, the polaron bandwidth is narrower than the phonon frequency. The upper part of the band has much less dispersion than the lower part but *with a substantial* Z_k. This indicates a distinct mechanism for the crossover as a function of $\vec{k}$. In the case of $\lambda=4.5$, the strong el-ph interaction leads to the well-known polaron band collapse and a significant suppression of Z_k at all k.

V. TOYOZAWA VARIATIONAL METHOD

Four decades ago, a simple and intuitive variational approach to the 1D polaron problem was proposed by Toyozawa.[36] This method has been successfully applied to various fields and revisited in a number of guises[37,38] throughout the years. It is generally believed to provide a qualitatively correct description of the polaron ground state, aside from predicting a spurious discontinuous change in the mass at intermediate coupling. We show below that although the Toyozawa wave function gives a good account of the ground state energy and the two-point functions, it fails to correctly describe the three-point functions.

The Toyozawa wave function is written as a product of coherent states,

$$|\Psi_T(k)\rangle=\sum_j e^{ikj}\ c_j^\dagger|0\rangle\prod_m |z_{j+m}\rangle, \tag{8}$$

where $|z_i\rangle$ is a coherent state of the phonon mode on site i. In the antiadiabatic limit $\omega/t\to\infty$, this wave function gives the exact solution $c_j^\dagger|0\rangle|z_j\rangle$, where $z_j=\lambda/\omega$ and the other z's are zero. For the general case, momentum $k=0$, the z's are real and symmetric: $z_{j+m}=z_{j-m}$. To determine the validity of the Toyozawa wave function, we probe the structure of the phonon cloud in the $k=0$ ground state by computing the following two- and three-point el-ph correlation functions:

$$\alpha_2(j)\equiv\langle c_0^\dagger c_0 a_j^\dagger a_j\rangle, \tag{9}$$

$$\alpha_3(j,m)\equiv\langle c_0^\dagger c_0 a_j^\dagger a_j a_m^\dagger a_m\rangle. \tag{10}$$

The z's in Eq. (8) are optimized so as to give a minimum energy. It can be proved that the optimal z's decay exponentially as a function of the el-ph separation. Thus they always give purely exponentially decaying two-point functions re-

TABLE II. A comparison of the ground-state energy E_0, two- and three-point el-ph correlation functions, and $Z_{k=0}$, evaluated by the present method, the Toyozawa method, equation (11), and Shore-Sander wave functions (Ψ^{IV} in Ref. 40). Parameters are $\lambda=1.2$, $\omega=1$, $t=1$, and $D=1$.

	E_0	$\alpha_2(0)$	$\alpha_3(1,2)$	$\alpha_3(1,-2)$	$Z_{k=0}$
This work	-2.69356579774920 . . .	0.40770	0.0004691	0.000005888	0.627322 . . .
Toyozawa	-2.662819	0.32527	0.0002142	0.0002142	0.65738
Eq. (11)	-2.671530	0.34240	0.0007649	0.000003244	0.64271
Shore and Sander	-2.685826	0.37780	0.0005572	0.0001132	0.63757

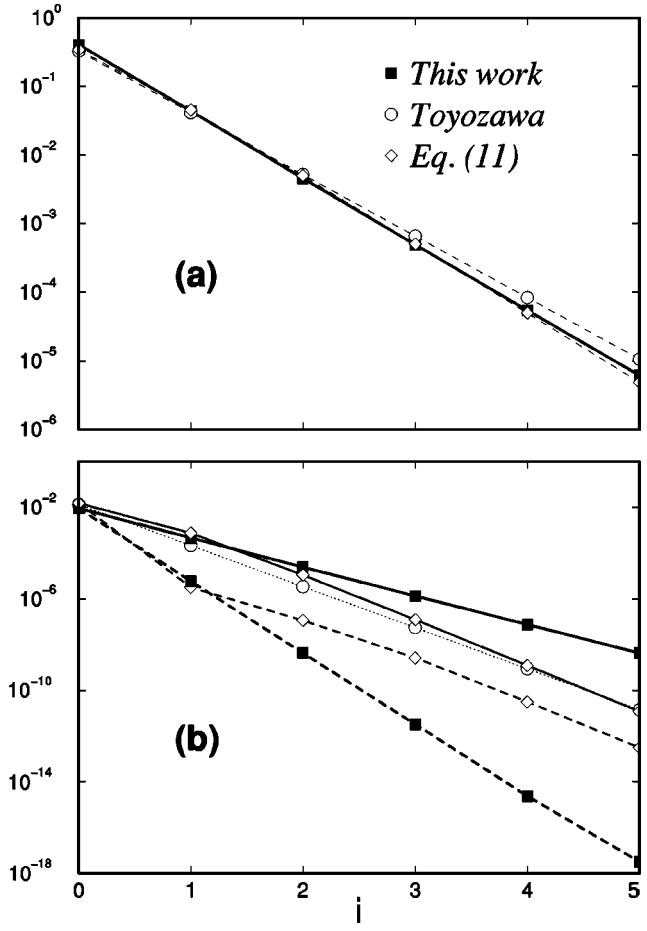

FIG. 11.

FIG. 11. (a) The two-point function $\alpha_2(j)$ is evaluated in one dimension by the present variational method (solid line with squares), the Toyozawa method (dashed line with circles), and the modified Toyozawa method [Eq. (11)] (dashed line with diamonds). (b) The three-point functions $\alpha_3(j,j+1)$ (solid lines) and $\alpha_3(j,-j-1)$ (dashed lines). The symbols are the same as in (a). Note that the plain Toyozawa method gives exactly the same results for the two three-point functions, which in fact differ widely. Parameters are $\omega=1.0$, $t=1.0$, and $\lambda=1.2$.

gardless of the el-ph coupling. This, however, is not true of the numerically exact results. Table II and Fig. 11 compare Toyozawa's results and the numerically exact results for intermediate coupling.[39] We note that the Toyozawa wave function gives reasonably accurate results for the ground-state energy, two-point functions, and $Z_{k=0}$. In Table II, the fractional error in energy is about 1% (with $z_{j+1}/z_j=0.35568$ and $z_0=0.57033$). However, it gives wildly inaccurate three-point functions. For example, Toyozawa's $\alpha_3(1,-2)$ is a factor of 36 too large and $\alpha_3(1,2)$ is a factor of 2 too small. Toyozawa's $\alpha_3(5,-6)$ is too large by six orders of magnitude. This failure indicates that the electron does not organize its surrounding phonon cloud in the way that Toyozawa suggested. Instead, by directly analyzing the exact ground-state wave function, we find that the electron organizes its surrounding phonons like a traveling salesman does, namely, the polaron favors the phonon configuration with a shorter creation path. (The length of the creation path is the number of off-diagonal operations, phonon creations and electron hops, required to create a state from the bare electron state. Shorter paths are favored at intermediate or weak el-ph coupling, although more on-site phonons can be favored at large coupling.) For example, we have

$$|\langle\Psi_0|c_0^\dagger a_0^\dagger|0\rangle|>|\langle\Psi_0|c_0^\dagger a_1^\dagger|0\rangle|>|\langle\Psi_0|c_0^\dagger a_2^\dagger|0\rangle|>\cdots$$

in the one-phonon subspace and

$$|\langle\Psi_0|c_0^\dagger a_0^\dagger a_0^\dagger|0\rangle|>|\langle\Psi_0|c_0^\dagger a_1^\dagger a_1^\dagger|0\rangle|>|\langle\Psi_0|c_0^\dagger a_1^\dagger a_{-1}^\dagger|0\rangle| > \cdots$$

in the two-phonon subspace. The amplitude attenuates rapidly as the phonon-creation path increases.

TABLE III. A partial list of the optimized phonon wave function z_j in Eq. (11).

Site j	z_j
-6	-0.12384D-03
-5	-0.39019D-03
-4	-0.11875D-02
-3	-0.32178D-02
-2	-0.48444D-02
-1	0.35290D-01
0	0.58515D+00
1	0.38153D+00
2	0.14043D+00
3	0.46112D-01
4	0.14632D-01
5	0.45908D-02
6	0.14349D-02

The numerically exact result in Fig. 11(b) shows that it is far more favorable to create two-phonon excitations on the same side of the electron than on opposite sides. Therefore, we propose to write a polaron as a sum of two asymmetric clouds, one extending like a comet tail primarily off to the right and the other extending to the left,

$$|\Psi_T'(k)\rangle=\sum_j e^{ikj}c_j^\dagger|0\rangle(\cdots|z_{j-2}\rangle|z_{j-1}\rangle|z_j\rangle|z_{j+1}\rangle|z_{j+2}\rangle\cdots + \cdots|z_{j+2}\rangle|z_{j+1}\rangle|z_j\rangle|z_{j-1}\rangle|z_{j-2}\rangle\cdots), \quad (11)$$

where $z_{j-m}\neq z_{j+m}$, and the normalization factor has been omitted. The optimized (minimum-energy) phonon wave function in Eq. (11) is strongly asymmetric, and in fact changes sign on one side, as shown in Table III. The main purpose of Eq. (11) is to investigate how the simplest asymmetric wave function improves the Toyozawa method. Shore and Sander have proposed a more complicated wave function $|\Psi_{SS}^{IV}\rangle$ which is a sum of the symmetric term in Eq. (8) and the two asymmetric terms in Eq. (11).[40] (Asymmetric wave functions were also considered in Ref. 37.) The number of independent variables in Ψ_T, Ψ_T', and Ψ_{SS}^{IV} is $\frac{1}{2}N$, N, and $\frac{3}{2}N$, respectively, where N is the number of sites that allow phonon excitations. The minimum energies from the

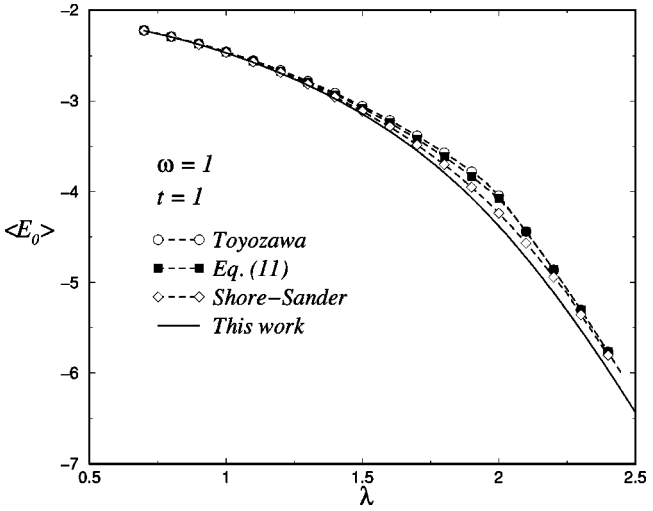

FIG. 12. A comparison of the ground-state energy as a function of the coupling constant from various variational approaches for $\omega=1$ and $t=1$.

above methods are compared in Fig. 12. It is clear that the energies are improved as we expand the variational space, $\Psi_T \subset \Psi_T' \subset \Psi_{SS}^{IV}$. The Shore-Sander method shows the most substantial improvement in the crossover regime. The comparison of other polaron properties is shown in Table II and Fig. 11. Our trial wave function $|\Psi_T'\rangle$ improves the energy by 30% and the $k=0$ Z factor by 50% compared to 75% and 66%, respectively, from the Shore-Sander wave function. In Fig. 11(a), Eq. (11) gives a more accurate two-point function $\alpha_2(j)$ than the original Toyozawa function. It similarly improves the other two-point function χ_j (not shown). Panel (b) shows two three-point functions, $\alpha_3(j,j+1)$ and $\alpha_3(j,-j-1)$. Due to its symmetric phonon cloud, the Toyozawa wave function must give exactly the same result for the two three-point functions. In contrast, the exact results show that $\alpha_3(j,j+1) \gg \alpha_3(j,-j-1)$. Equation (11) gives the correct behavior of the two three-point functions on nearby sites, but loses quantitative accuracy in the tails. Although the Shore-Sander energy is better than that of Eq. (11), the Shore-Sander three-point functions are actually worse. The simplest attempt $|\Psi_T'\rangle$ to correct the identified shortcomings in the Toyozawa variational wave function appears to be a step in the right direction, although not as quantitatively accurate for most properties as variational methods with more parameters.[17,41]

VI. CONCLUSION

In summary, we have performed extensive numerical studies of the Holstein polaron in spatial dimensions 1 through 4. The numerical method used adds basis states to the Hilbert space in an efficient order, resulting in an error that scales as a power of the size of the Hilbert space $N_{st}^{-\theta}$, where θ is a nonuniversal exponent ≈ 3 at intermediate coupling in 1D, and ≈ 1.6 in 3D. This is a qualitative improvement over standard exact diagonalization, which requires exponential effort to achieve a given accuracy. Using modest computational resources, we obtain by far the most accurate polaron energies and wave functions available from 1D to 4D at intermediate coupling.

Previously, a thorough investigation of the dimensionality effect, including correlation functions, was out of reach of numerical methods. The main findings of the dimensionality effects on the Holstein polaron are summarized as follows: The crossover from a quasifree to a large effective mass is found to be much sharper in higher dimensions. As was recognized previously, there is no symmetry-breaking self-trapping transition for finite parameters in any dimension, as suggested by adiabatic theory (although there is a phase transition in the first excited state[21]). See also Ref. 29. Our results for m^* agree with QMC, although there is a discrepancy with DMRG in $D>1$. The electron-phonon correlation functions decay significantly faster in higher than lower dimensions. This implies a shorter el-ph correlation length in large dimensions and leads to a diminishing difference between the inverse effective mass m_0/m^* and the wave function renormalization $Z_{\vec{k}=0}$ as D increases. The DMFT approach thus gives better results in higher dimensions. Our comparison shows that DMFT gives qualitatively correct results for the effective mass, mean phonon number, and on-site phonon distortion in the intermediate- to strong-coupling regime. We also examine the comb-basis approach, which limits the el-ph correlation to the on-site level as DMFT does. The discrepancy between the comb basis and the full basis decreases slowly as D increases.

Finally, our approach is compared to the well-known Toyozawa variational method. We quantitatively examine the method in the intermediate-coupling regime. Overall, the Toyozawa wave function gives reasonably accurate energy and two-point functions, but fails seriously for the three-point functions. (The numerically exact three-point functions are quite different for excitations on opposite sides of the electron compared to the same side, whereas the Toyozawa wave function predicts that they are identical.) We propose an improved variational wave function, a sum of two asymmetric phonon clouds [Eq. (11)], which gives improved three-point functions, and somewhat more accurate results for the energy, Z factor, and two-point el-ph correlation functions.

For all the polaron features calculated, the present numerical approach compares favorably to other numerical methods in terms of accuracy, ease of implementation, and the ability to compute ground- and excited-state energies and correlation functions. It can also be directly applied to study the effects of dimensionality on other interesting problems, such as the Fröhlich model or extended Holstein model with longer-range electron-phonon interactions, and to bipolaron problems.

ACKNOWLEDGMENTS

The authors are grateful to S. Ciuchi, E. Jeckelmann, and P. Kornilovitch for discussions and permission to use their data, and to J. E. Gubernatis and K. K. Loh for valuable discussions. This work was supported by the U.S. Department of Energy and by Los Alamos LDRD.

[1] G. M. Zhao, V. Smolyaninova, W. Prellier, and H. Keller, Phys. Rev. Lett. **84**, 6086 (2000), and references therein.
[2] I. H. Campbell and D. L. Smith, Solid State Phys. **55**, 1 (2001).
[3] *Lattice effects in High-T_c Superconductors*, edited by Y. Bar-Yam, T. Egami, J. Mustre de Leon, and A. R. Bishop (World Scientific, Singapore, 1992); A. S. Alexandrov and N. F. Mott, *Polarons and Bipolarons* (World Scientific, Singapore, 1995).
[4] A. Lanzara, P. V. Bodganov, X. J. Zhou, S. A. Kellar, D. L. Feng, E. D. Lu, T. Yoshida, H. Eisaki, A. Fujimori, K. Kishio, J.-I. Shimoyama, T. Noda, S. Uchida, Z. Hussain, and Z.-X. Shen, Nature (London) **412**, 510 (2001).
[5] E. I. Rashba, in *Modern Problems in Condensed Matter Sciences, Vol. 2, Excitons*, edited by E. I. Rashba and M. D. Sturge (North Holland, Amsterdam, 1982), p. 543.
[6] T. Holstein, Ann. Phys. (N.Y.) **8**, 325 (1959).
[7] J. Appel, Solid State Phys. **21**, 193 (1968).
[8] A. S. Alexandrov, V. V. Kabanov, and D. K. Ray, Phys. Rev. B **49**, 9915 (1994).
[9] G. Wellein, H. Röder, and H. Fehske, Phys. Rev. B **53**, 9666 (1996).
[10] E. V. L. de Mello and J. Ranninger, Phys. Rev. B **55**, 14 872 (1997).
[11] G. Wellein and H. Fehske, Phys. Rev. B **56**, 4513 (1997); H. Fehske, J. Loos, and G. Wellein, Z. Phys. B: Condens. Matter **104**, 619 (1997).
[12] M. Capone, W. Stephan, and M. Grilli, Phys. Rev. B **56**, 4484 (1997).
[13] C. Zhang, E. Jeckelmann, and S. R. White, Phys. Rev. B **60**, 14 092 (1999).
[14] P. E. Kornilovitch, Phys. Rev. Lett. **81**, 5382 (1998).
[15] P. E. Kornilovitch, Phys. Rev. B **60**, 3237 (1999).
[16] E. Jeckelmann and S. R. White, Phys. Rev. B **57**, 6376 (1998).
[17] A. W. Romero, D. W. Brown, and K. Lindenberg, J. Chem. Phys. **109**, 6540 (1998).
[18] D. Emin and T. Holstein, Phys. Rev. Lett. **36**, 323 (1976).
[19] Y. Toyozawa and Y. Shinozuka, J. Soc. Jpn. **48**, 472 (1980).
[20] A. H. Romero, D. W. Brown, and K. Lindenberg, Phys. Rev. B **60**, 14 080 (1999); Phys. Lett. A **266**, 414 (2000).
[21] J. Bonča, S. A. Trugman, and I. Batistić, Phys. Rev. B **60**, 1633 (1999).
[22] Problems with other types of electron-phonon coupling and lattices, as well as the two-electron (bipolaron) problem, can be solved by similar methods.
[23] For strong electron-phonon coupling, it is sometimes advantageous to add more phonon basis states very near to the electron, called a ''tower.'' Even with a tower, convergence is slower at strong coupling, corresponding to a shallower slope in Fig. 2.
[24] H. Fehske (private communication).
[25] B. Gerlach and H. Löwen, Rev. Mod. Phys. **63**, 63 (1991); Phys. Rev. B **35**, 4291 (1987).
[26] S. A. Trugman, J. Bonča, and L. C. Ku, Int. J. Mod. Phys. B **15**, 2707 (2001).
[27] J. Bonča and S. A. Trugman, Phys. Rev. B **64**, 094507 (2001).
[28] H. Fehske, J. Loos, and G. Wellein, Phys. Rev. B **61**, 8016 (2000).
[29] S. Ciuchi, F. de Pasquale, S. Fratini, and D. Feinberg, Phys. Rev. B **56**, 4494 (1997), and references therein.
[30] J. K. Freericks, M. Jarrell, and D. J. Scalapino, Phys. Rev. B **48**, 6302 (1993).
[31] S. Ciuchi, F. de Pasquale, and D. Feinberg, Europhys. Lett. **30**, 151 (1995).
[32] A. H. Romero, D. W. Brown, and K. Lindenberg, Phys. Lett. A **254**, 287 (1999).
[33] The nearest-neighbor correlation $\chi(1)/\chi(0)$ was calculated at finite temperature by QMC. See H. De Raedt and A. Lagendijk, Phys. Rev. Lett. **49**, 1522 (1982).
[34] All presented el-ph correlation functions are evaluated for wave functions that are normalized to one electron per site. For conventional normalization, there would be an additional $1/N$ factor, where N is the number of sites in the system.
[35] The error in the flattened band is about 2.1% for the 3D polaron. In the weak-coupling regime, the extent of the el-ph correlations at $k=\pi$ is much larger than at $k=0$. For the 1D polaron, the el-ph correlations decay exponentially at all k for all parameters; the polaron and additional phonon are bound at $k=\pi$. It is not clear that this is the case in three dimensions.
[36] Y. Toyozawa, Prog. Theor. Phys. **26**, 29 (1961).
[37] G. Venzl and S. F. Fischer, J. Chem. Phys. **81**, 6090 (1984); Phys. Rev. B **32**, 6437 (1985).
[38] Y. Zhao, D. W. Brown, and K. Lindenberg, J. Chem. Phys. **107**, 3159 (1997).
[39] A comparison of energies obtained by a wider variety of methods is contained in Ref. 17. Note that what is referred to as the ''Toyozawa variation'' in that reference is a more sophisticated trial function than what we call the Toyozawa wave function [Eq. (8)].
[40] H. B. Shore and L. M. Sander, Phys. Rev. **7**, 4537 (1973).
[41] A series of studies on improving the Toyozawa variational method can be found in Refs. 17 and 38, and in Y. Zhao, D. W. Brown, K. Lindenberg, J. Chem. Phys. **106**, 5622 (1997).